RSC Advances

This article can be cited before page numbers have been issued, to do this please use: S. Xue, G. Chen, Z. Long, Y. Zhou and J. Wang, *RSC Adv.*, 2015, DOI: 10.1039/C4RA15921G.

ROYAL SOCIETY OF CHEMISTRY

www.rsc.org/advances

View Article Online
DOI: 10.1039/C4RA15921G

RSC Advances

RSCPublishing

ARTICLE

Efficient and recyclable multi-cationic polyoxometalate-based hybrid catalyst for heterogeneous cyclohexane oxidation with H_2O_2

Cite this: DOI: 10.1039/xoxxoooooox

Received ooth January 2014,
Accepted ooth January 2014

DOI: 10.1039/xoxxoooooox

www.rsc.org/

Shuang Xue, Guojian Chen, Zhouyang Long, Yu Zhou*, and Jun Wang*

A polyoxometalate-based organic-inorganic hybrid was prepared by ionic self-assembly of the ionic liquid precursor N,N'-bis-2-aminoethyl-4,4'-bipyridinium dibromide dihydrobromide ([DPyAM]Br_2 2HBr) with the Keggin-structured V-substituted polyoxometalate $H_5PMo_{10}V_2O_{40}$ (H_5PMoV_2). The composition, electronic and porous structure of the resultant hybrid $[DPyAM(H_2)]_{1.25}PMoV_2$ were demonstrated by CHN elemental analysis, ^{1}H NMR, TG, SEM, XRD, FT-IR, UV-vis, ESR, and nitrogen sorption techniques. Catalytic tests showed that the hybrid was a highly active heterogeneous catalyst for cyclohexane oxidation with hydrogen peroxide, giving a yield to KA oil (mixture of cyclohexanol and cyclohexanone) of ca. 29.4% with high turnover number (TON) of 2940 using very low catalyst dosage (0.01 mol% vs. substrate). The catalyst can be conveniently separated by filtration and reused without observing significant decrease in activity. Influences of reaction conditions were systematically investigated and a possible catalysis mechanism was proposed for understanding the highly efficient heterogeneous catalytic behavior.

1. Introduction

Catalysis technology for efficient and selective conversion of inactive C-H bonds in saturated hydrocarbons into various valuable products is an important issue in chemical industry. Though many efforts have been made in this context, developing efficient catalysts still remains a major challenge so far.[1-4] One particularly difficult case is the oxidation of cyclohexane into KA oil (mixture of cyclohexanol and cyclohexanone); the products are commodity chemicals of large demand.[5] The industrial process to produce KA oil involves a homogeneous cobalt catalyst with a low yield (ca. 4%), which needs a considerably high temperature of 150 ^oC.[6,7] For the purpose of achieving a sustainable green process, exploration of new catalysts is greatly demanded, especially the easily isolatable and steadily reusable heterogeneous catalysts.

A large number of catalysts have been attempted for the oxidation of cyclohexane, such as metal oxides, molecular sieves, metal substituted polyoxometalates (POMs), metalloporphyrin complexes, and so on.[8-10] Actually, as a class of distinctive inorganic transition metal-oxygen clusters with tunable architectures, POMs have been extensively studied as the catalysts for many oxidative organic reactions due to the inherent redox property of the high valence metal ions in POM frameworks, among which oxidation of alkanes has also been investigated over POM-based catalysts.[11] For the oxidation of cyclohexane with H_2O_2, the Keggin-structured POM-anions like $[PW_{11}O_{39}]^{7-}$, $[PW_{11}Fe(H_2O)O_{39}]^{4-}$, and divanadium-substituted phosphotungstate $[\gamma\text{-}H_2PV_2W_{10}O_{40}]^{3-}$ have been reported[12,13] as promising catalysts. However, most of the early reported catalytic systems are homogeneous due to the soluble nature of POMs in (highly) polar reaction media. For heterogenization of POMs catalysts, tetrabutyl-ammonium modified transition metals (V, Cu, Co or Fe) substituted polyoxometalates and cesium polyoxotungstates were immobilized on MCM-41 or SiO_2;[14-16] however, that supporting strategy usually involves complex preparation procedures. Up to date, it still has a long march to obtain a simply prepared and recyclable active heterogeneous catalyst for cyclohexane oxidation.

Herein, a new strategy for enhancing the reactivity of cyclohexane oxidation is developed by employing ionic liquid cation-paired POM catalyst. In POMs chemistry, incorporation of organic units to POM-anions has been an effective approach to broaden the utilizations of POM-derived materials,[17] wherein the functionalized organic ionic liquid (IL) cations are among the most effective modifiers to pair POM-anions. By "task-specific" designing of functional IL-cations for pairing suitable POMs, various functionalized IL-POM hybrids have been prepared and acted as effective, recoverable and reusable catalysts for oxidative organic transformations.[18-22] Taking account of the well-known highly active Keggin-structured V-containing POMs for catalyzing oxidative organic reactions, in this work we attempt to prepare an IL-cation-paired V-POM-based organic-inorganic hybrid catalyst for heterogeneous oxidation of cyclohexane with H_2O_2, which to our knowledge has not been reported as yet. The ionic liquid precursor N,N'-bis-2-aminoethyl-4,4'-bipyridinium dibromide dihydrobromide is designed and prepared, which reacts with the POM of phosphovanadomolybdic acid $H_5PMo_{10}V_2O_{40}$ to generate the novel IL-cation-paired POM-based ionic hybrid compound. Systematical investigations for catalyzing the oxidation of

cyclohexane with H_2O_2 demonstrate the excellent heterogeneous behaviors of this newly obtained hybrid. The influence of various parameters are measured, such as amounts of catalyst, oxidant and solvent, reaction time, and the type of IL-cations. Also, the mechanism of the cyclohexane oxidation catalyzed by this hybrid catalyst is proposed.

2. Experimental section

2.1. Materials and methods

All the chemicals were analytical grade and used as received. The CHN elemental analysis was performed on an elemental analyzer Vario EL cube. TG analysis was carried out with a STA409 instrument in dry air at a heating rate of 10 $^oC\ min^{-1}$. BET surface area was measured at the temperature of liquid nitrogen (77 K) using a BELSORP-MINI analyzer and the sample was degassed at 150 ^oC for 3 hours to a vacuum of 10^{-3} Torr before analysis. SEM image was obtained on a HITACHI S-4800 field-emission scanning electron microscope. ^1H NMR spectra were measured with a Bruker DPX 500 spectrometer at ambient temperature in D^6-DMSO using TMS as internal reference. X-ray diffraction (XRD) measurements were collected on a SmartLab diffractometer from Rigaku equipped with a 9 kW rotating anode Cu source at 40 kV and 20 mA, from 5^o to 50^o with a scan rate of 0.2^o s^{-1}. FT-IR spectra were recorded on a Nicolet iS10 FT-IR instrument (KBr discs) in the region 4000-400 cm^{-1}. Solid UV-vis spectra were measured with a SHI-MADZU UV-2600 spectrometer and $BaSO_4$ was used as an internal standard. ESR spectra were recorded on a Bruker EMX-10/12 spectrometer at the X-band.

2.2. Synthesis of catalysts

Keggin-structured double V-containing heteropolyacid $H_5PMo_{10}V_2O_{40}$ (H_5PMoV_2) was prepared according to the procedure described before.[23] The details were as follows. MoO_3 (16.59 g, 0.115 mol) and V_2O_5 (2.10 g, 0.0115 mol) were mixed with deionized water (250 mL) in a flask reactor equipped with a water-cooled condenser and magnetic stirrer, which was heated up to 120 ^oC for reflux under vigorous stirring. The concentrated H_3PO_4 (85 wt%, 1.33 g, 0.0115 mol) in water (10 mL) was drop-wise added into the above mixture within 30 min. With a further stirring for 24 h, a clear orange-red solution appeared. After the solution was cooled to room temperature, a fine orange powder was produced by vacuum drying at 50 ^oC for 24 h. The final product H_5PMoV_2 was obtained by recrystallizing the powdered solid in deionized water and another vacuum drying at 50 ^oC for 24 h.

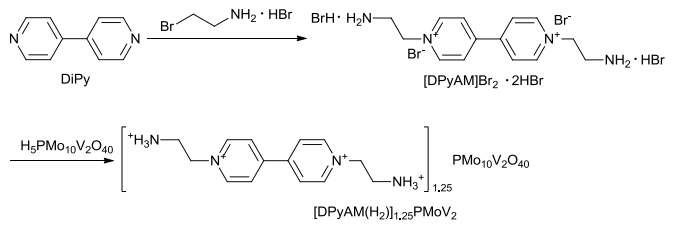

Scheme 1 Synthesis of the multi-cationic IL-POM catalyst $[DPyAM(H_2)]_{1.25}PMoV_2$.

The preparation of catalyst $[DPyAM(H_2)]_{1.25}PMoV_2$ was shown in Scheme 1. The ionic liquid precursor, N,N'-bis-2-aminoethyl-4,4'-bipyridinium dibromide dihydrobromide ($[DPyAM]Br_2\ 2HBr$), was prepared according to our previous report.[24] 4,4-Bipyridyl (0.02 mol) and 2-bromoethylamine hydrobromide (0.04 mol) were dissolved in acetonitrile (50 mL) at 80 ^oC and keeping for 12 h with stirring. Then, the precipitate was filtered, washed with acetonitrile, and dried to afford $[DPyAM]Br_2\ 2HBr$ as a yellow solid. Elemental analysis calcd (wt%): C 29.71, H 3.92, N 9.90; found: C 29.20, H 3.95, N 9.74. ^1H NMR (300 MHz, D^6-DMSO, TMS) (Fig. S1, Supporting Information) δ (ppm) = 3.26-3.89 (m, 4H, -CH_2), 5.09 (m, 4H, -CH_2), 8.34 (d, 4H, -NH_2), 8.99 (d, 4H, -CH), 9.51 (d, 4H, -CH). The catalyst $[DPyAM(H_2)]_{1.25}PMoV_2$ was synthesized through the reaction of above IL precursor and H_5PMoV_2. $[DPyAM]Br_2\ 2HBr$ (1.25 mmol) was added to an aqueous solution of H_5PMoV_2 (1.0 mmol), and then the mixture was stirred at room temperature for 24 h. The formed yellow-green precipitate $[DPyAM(H_2)]_{1.25}PMoV_2$ was filtered and washed with water for three times, followed by drying in a vacuum.

Other analogues of POM salts [aminoethyl-pyridinium]$_5PMo_{10}V_2O_{40}$ ($[PyAM]_5PMoV_2$), [N-butyronitrile pyridine]$_5PMo_{10}V_2O_{40}$ ($[PyCN]_5PMoV_2$), [1-butyl-3-methylimidazolium]$_5PMo_{10}V_2O_{40}$ ($[MimC_4]_5PMoV_2$), [1-butyronitrile-3-methylimidazolium]$_5PMo_{10}V_2O_{40}$ ($[MimCN]_5PMoV_2$), [N,N'-bis(carboxymethyl) 4,4'-bipyridinium]$_5PMo_{10}V_2O_{40}$ ($[DPyCOOH]_{2.5}PMoV_2$), [N,N'-bis(3-cyanopropyl) 4,4'-bipyridinium]$_5PMo_{10}V_2O_{40}$ ($[DPyCN]_{2.5}PMoV_2$), [N,N'-dibutyl 4,4'-bipyridinium]$_5PMo_{10}V_2O_{40}$ ($[DPyC_4]_{2.5}PMoV_2$) and [1,1'-(butane-1,4-diyl) bis(3-methylimidazolium)]$_5PMo_{10}V_2O_{40}$ ($[DMim]_{2.5}PMoV_2$) were prepared based on similar procedures by reacting H_5PMoV_2 with the corresponding IL precursors, using the stoichiometric molar ratio of the precursors. The details of the synthesis and structure formulas were described in the Supporting Information (Scheme S1). Elemental analysis results: calcd for $[PyAM]_{3.1}H_{1.9}PMo_{10}V_2O_{40}\ 4H_2O$ (wt%): C 11.91, H 2.03, N 3.97; found: C 12.05, H 2.15, N 3.89; calcd for $[PyCN]_{4.3}H_{0.7}PMo_{10}V_2O_{40}\ H_2O$ (wt%): C 19.50, H 2.11, N 5.05; found: C 19.47, H 2.09, N 4.86; calcd for $[MimC_4]_{4.3}H_{0.7}PMo_{10}V_2O_{40}\ 2H_2O$ (wt%): C 17.45, H 2.95, N 5.09; found: C 17.49, H 2.78, N 4.97; calcd for $[MimCN]_{3.1}H_{1.9}PMo_{10}V_2O_{40}$ (wt%): C 11.91, H 2.03, N 3.97; found: C 12.05, H 2.15, N 3.89; calcd for $[DPyCOOH]_2HPMo_{10}V_2O_{40}\ 6H_2O$ (wt%): C 14.07, H 1.73, N 2.34; found: C 14.04, H 1.71, N 2.50; calcd for $[DPyCN]_{1.4}H_{2.2}PMo_{10}V_2O_{40}\ 5H_2O$ (wt%): C 13.55, H 1.81, N 3.51; found: C 13.56, H 1.62, N 3.47; calcd for $[DPyC_4]_{2.2}H_{0.6}PMo_{10}V_2O_{40}\ 3H_2O$ (wt%): C 19.97, H 2.70, N 2.59; found: C 20.00, H 2.73, N 2.38; calcd for $[DMim]_{2.3}H_{0.4}PMo_{10}V_2O_{40}\ H_2O$ (wt%): C 14.69, H 2.16, N 5.71; found: C 14.62, H 2.15, N 5.41.

2.3. Catalytic tests

The catalytic oxidation of cyclohexane with hydrogen peroxide as the oxidant was performed under a magnetic stirring thermostatted glass vessel reactor. In a typical experimental procedure, the reaction mixtures were prepared as follows: cyclohexane (5 mmol), catalyst (2 μmol), acid additive (pyrazine-2,3-dicarboxylic acid shorten as 2,3-PDCA, 0.3 mmol), and 5 mL of acetonitrile was used as solvent. Acetonitrile was chosen as the solvent in our system, owing to its high resistance to oxidizing agents and also in view of the good solubility of the substrate and organic products. Then,

View Article Online
DOI: 10.1039/C4RA15921G
ARTICLE

aqueous H_2O_2 (30 wt%, 10 mmol) was drop-wise added into the reactor within 30 min (to minimise H_2O_2 decomposition) under stirring, and the reaction time was counted after the addition of H_2O_2. The typical reaction temperature was 80 ^oC and reaction time was 6 h. The hot filtration test for removing the solid catalyst was conducted at 0.5 h, with the filtrate being further reacted for another 5.5 h. In the experiments with radical traps, $CBrCl_3$, butylated hydroxytoluene (BHT, carbon radical trap) or Ph_2NH (oxygen radical trap) were used in a stoichiometric amount relative to substrate or H_2O_2.[25]

After the reaction, 2.5 mmol of methylbenzene (internal standard) was added. Excess of triphenylphosphine (PPh_3) was added into the obtained mixture before GC analysis, in order to reduce the formed cyclohexyl hydroperoxide to the corresponding alcohol, and hydrogen peroxide to water, following a method developed by Shul'pin.[26] Thus, all catalytic runs were analyzed after the addition of PPh_3 for accurate determination of the final oxygenated products, cyclohexanol and cyclohexanone. After stirring the final reaction mixture for 10 min, a sample was taken and then analyzed by gas chromatography (GC, Agilent GC 7890B) equipped with a hydrogen flame ionization detector and capillary column (HP-5, 30 m × 0.25 mm × 0.25 μm). Apart from cyclohexanol and cyclohexanone, no other products were detected by GC analysis. Authentic samples of oxygenated products were used to attribute the peaks in chromatograms.

At the end of the reaction, the catalyst was separated from the reaction mixture by filtration and was thoroughly washed several times with distilled water and ethanol. Then, the catalyst was dried at 80 ^oC for 4 h in vacuum, and reused in the next run.

3. Results and discussion

3.1. Structure characterization

The elemental analysis for the ionic hybrid $[DPyAM(H_2)]_{1.25}PMoV_2$ finds C: 10.13%, N: 3.14%, and H: 1.84% (by weight percentage), reasonably in agreement with the calculated value of C: 10.30%, N: 3.43%, and H: 1.36%. The TG analysis for $[DPyAM(H_2)]_{1.25}PMoV_2$ (Fig. 1A) demonstrates a stable structure up to 230 ^oC. The slight weight loss at the early heating stage before 230 ^oC is due to the release of moisture and constitutional water, while the drastic weight loss above 230 ^oC is attributed to the decomposition of the organic moiety plus collapse of the inorganic Keggin structure into P_2O_5, MoO_3, and V_2O_5. The weight loss of ca. 6.9 wt% in the range of 230~350 ^oC is probably due to the decomposition of 4,4'-dipyridinium framework, and that of ca. 7.5 wt% in the range of 350~400 ^oC is attributed to the decomposition of the remaining organic moiety. The total weight loss in the range of 230~400 ^oC is ca. 14.4 wt%, close to the data of 15.1 wt% calculated according to the formula $[DPyAM(H_2)]_{1.25}PMoV_2$. ^1H NMR (300 MHz, D^6-DMSO, TMS) (Fig. S2) shows δ (ppm) = 3.65 (m, 4H, $-CH_2$), 5.11 (m, 4H, $-CH_2$), 8.08 (d, 4H, $-NH_2$), 8.89 (d, 4H, -CH), 9.37 (d, 4H, -CH). All the above results support the chemical structure of $[DPyAM(H_2)]_{1.25}PMoV_2$ that is composed of the IL-cation $DPyAM(H_2)^{4+}$ and the POM-anion $PMoV_2^{5-}$.

The SEM image for $[DPyAM(H_2)]_{1.25}PMoV_2$ in Fig. 1B shows the rod-like primary particles with sizes in diameter 150-200 nm and length up to 500-700 nm. These small rods are loosely packed to form secondary particles sized in micrometer level. Fig. 1C and D display the nitrogen sorption result for $[DPyAM(H_2)]_{1.25}PMoV_2$. The nitrogen sorption isotherm is type IV, suggesting a mesoporous structure. The pore size distribution curve presents wide pore size distribution from several to dozens of nanometers. The results indicate that $[DPyAM(H_2)]_{1.25}PMoV_2$ has a moderate BET surface area of 21.3 $m^2\ g^{-1}$ with an average pore diameter of 25.1 nm, consistent with that of our previously reported mesoporous IL-POM hybrid materials[20]. The specific surface area is mainly resulted by the packing of the small rod-like particles reflected in the above SEM image.

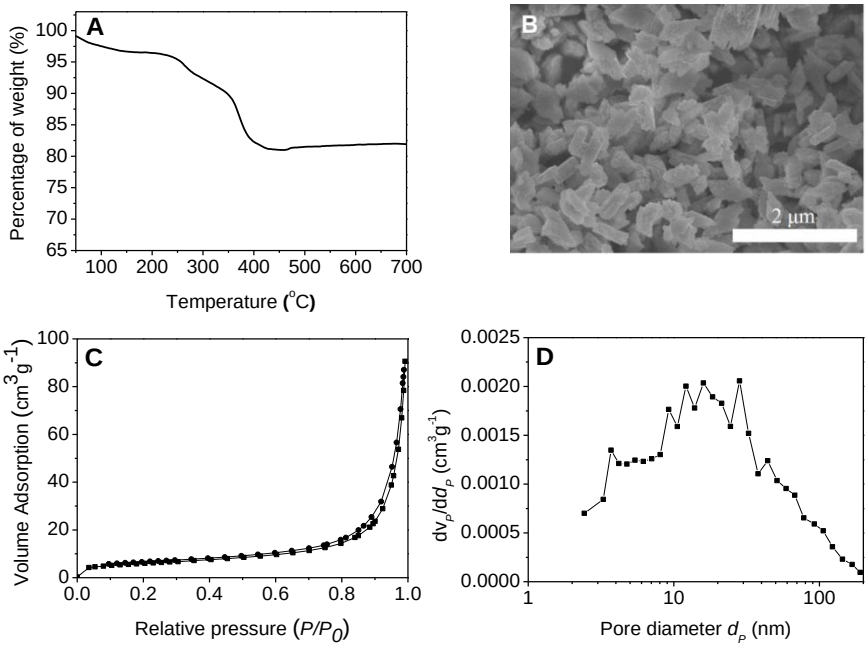

Fig. 1 TG curve (A), SEM image (B), N_2 adsorption-desorption isotherm (C) and BJH pore size distribution (D) of the hybrid $[DPyAM(H_2)]_{1.25}PMoV_2$.

View Article Online
DOI: 10.1039/C4RA15921G
RSC Advances

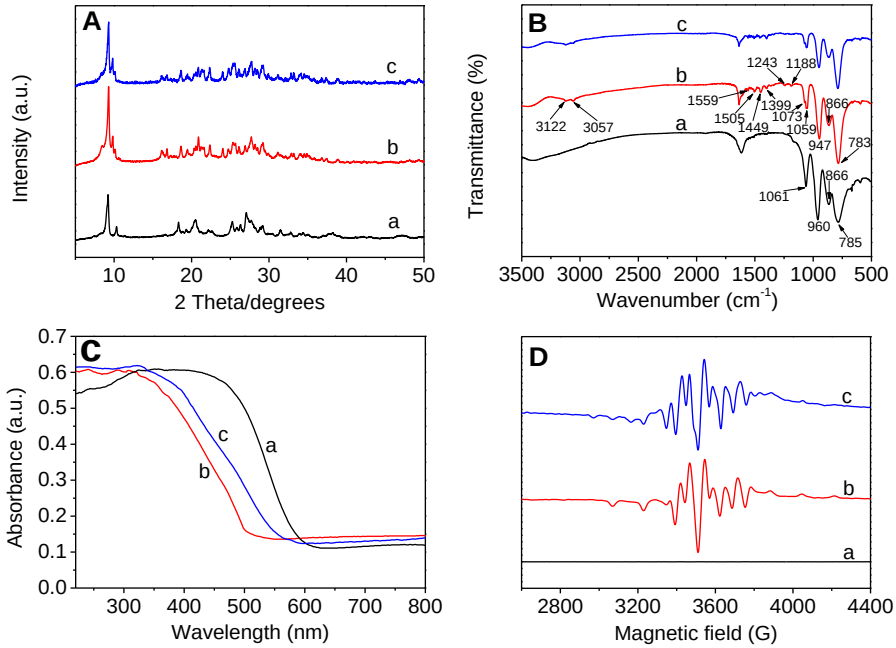

Fig. 2 XRD patterns (A), FT-IR spectra (B), UV-vis spectra (C) and ESR spectra (D) of a) H_5PMoV_2, b) fresh $[DPyAM(H_2)]_{1.25}PMoV_2$ and c) recycled $[DPyAM(H_2)]_{1.25}PMoV_2$.

Spectral characterizations for $[DPyAM(H_2)]_{1.25}PMoV_2$ and its POM parent H_5PMoV_2 are illustrated in Fig. 2. In XRD patterns (Fig. 2A), pure H_5PMoV_2 presents a set of diffraction peaks belonging to triclinic crystal system.[27] Compared to the parent, $[DPyAM(H_2)]_{1.25}PMoV_2$ preserves the similar strong Bragg peaks (2θ = 9.3, 9.8, 18.6, 20.9 and 27.7°) with slight shifts of peak locations, suggesting the retaining of the triclinic crystal structure.[28] Some variations of the latter may arise from the slight change of the long-range order of the original triclinic crystal lattice for the secondary structure of the POM unit when replacing the counter protons of H_5PMoV_2 with the larger IL-cations. In FT-IR spectra (Fig. 2B), H_5PMoV_2 shows the vibration bands assigned to the Keggin anion locating at 1061, 960, 866, and 785 cm^{-1}, corresponding to the asymmetric stretching vibration of the central oxygen (P-O) for PO_4 tetrahedron, terminal oxygen (Mo=O), inter- (Mo-O_b-Mo) and intra-octahedral oxygen (Mo-O_c-Mo), respectively.[29] For $[DPyAM(H_2)]_{1.25}PMoV_2$, the four Keggin-structured bands are apparent, revealing the well retain of the parent POM structure. The observations of slight shifts of the peak locations and the splitting of P-O vibration into two branches at 1073 and 1059 cm^{-1} imply the strong ionic interactions between the IL-cation and POM-anion.[30] Meanwhile, the ionic hybrid presents several characteristic bands index of the organic cations, including C-H stretching vibrations (3122 and 3057 cm^{-1}) plus C=C stretching vibrations (1559 and 1505 cm^{-1}) in the pyridine ring, C-H bending vibrations in methylene (1449 and 1399 cm^{-1}) and C-N stretching vibration (1243 and 1188 cm^{-1}).[18,31] The IR results confirm that the IL-POM hybrid $[DPyAM(H_2)]_{1.25}PMoV_2$ is composed of the ionic linked IL-cations and Keggin-structured POM-anions.

Moreover, in UV-vis spectra (Fig. 2C), the broad absorption band at 400 nm detected for H_5PMoV_2 is assigned to the charge transfer $O^{2-}\rightarrow V^{5+}$ in Keggin POM-anion.[32] In contrast, for $[DPyAM(H_2)]_{1.25}PMoV_2$, the band shifts to 310 nm , which can be assigned to the stronger charge transfer aided by the neighboring IL-cations, as have been previously discribed.[33] The charge transfer behavior in $[DPyAM(H_2)]_{1.25}PMoV_2$ is further evidenced by comparing the ESR curve of $[DPyAM(H_2)]_{1.25}PMoV_2$ with that of the parent H_5PMoV_2 (Fig. 2D). The ESR signals for H_5PMoV_2 are silent but those for $[DPyAM(H_2)]_{1.25}PMoV_2$ are sharp and strong, indicating the coexistence of V^{5+}/V^{4+} species in $[DPyAM(H_2)]_{1.25}PMoV_2$.[34]

3.2. Catalytic oxidation of cyclohexane

The hybrid $[DPyAM(H_2)]_{1.25}PMoV_2$ was tested as heterogeneous catalyst for the oxidation of cyclohexane by aqueous H_2O_2 (30 wt%) into KA oil (cyclohexanol + cyclohexanone) with acetonitrile as the solvent. Scheme 2 illustrates the oxidation process, in which the oxygenation of cyclohexane gives rise to the formation of alkyl hydroperoxide as the intermediate product that is further decomposed to yield stable products, cyclohexanol and cyclohexanone.

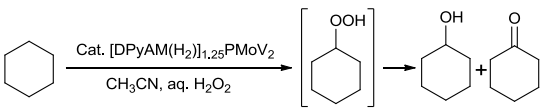

Scheme 2 Oxidation of cyclohexane with H_2O_2 catalyzed by $[DPyAM(H_2)]_{1.25}PMoV_2$.

As shown in Table 1, both the IL precursor $[DPyAM]Br_2$·2HBr and the V-free POM counterpart $H_3PMo_{12}O_{40}$ cannot give any alkane oxidation products, similar to the non-catalysis system (entries 1-3). The parent POM catalyst H_5PMoV_2 offers a considerable total (cyclohexanol + cyclohexanone) product yield of 27.8% (entry 4), suggesting that the vanadium ions in the POM-anion framework are catalytically active centers for this oxidative reaction. Nonetheless, H_5PMoV_2 results in a homogeneous catalysis with difficulty in catalyst isolation. The multi-cationic hybrid

View Article Online
DOI: 10.1039/C4RA15921G
RSC Advances ARTICLE

Table 1 Catalytic performance of various catalysts for the oxidation of cyclohexane with H_2O_2[a]

Entry	Catalyst	Phenomenon	Yield[b][%]			Total TON[c]
			$C_6H_{11}OH$	$C_6H_{10}O$	Total	
1	-	-	-	-	0	-
2	$[DPyAM]Br_2$ 2HBr	homogeneous	-	-	0	-
3	$H_3PMo_{12}O_{40}$	homogeneous	-	-	0	-
4	H_5PMoV_2	homogeneous	21.5	6.3	27.8	695
5	$[DPyAM(H_2)]_{1.25}PMoV_2$	heterogeneous	25.3	6.6	31.9	798
6[d]	$[DPyAM(H_2)]_{1.25}PMoV_2$	heterogeneous	25.8	3.6	29.4	2940
7[e]	$[DPyAM(H_2)]_{1.25}PMoV_2$	heterogeneous	-	-	0	-

[a] Reaction conditions (unless stated otherwise): cyclohexane (5 mmol), catalyst (2 μmol), 30% H_2O_2 (10 mmol), 2,3-PDCA (0.3 mmol), CH_3CN (5 mL), 80 °C, 6 h. Yields, TONs are determined by GC analysis (upon treatment with PPh_3). [b] Molar yield (%) based on substrate: moles of product (cyclohexanol + cyclohexanone) per 100 mol of cyclohexane. [c] Turnover number: moles of product (cyclohexanol + cyclohexanone) per mol of catalyst. [d] 0.5 μmol catalyst. [e] In the presence of radical traps ($CBrCl_3$, butylated hydroxytoluene or Ph_2NH).

$[DPyAM(H_2)]_{1.25}PMoV_2$ leads to a liquid-solid heterogeneous system, exhibiting 31.9% overall product yield with a turnover number (TON) of 798 (entry 5), which is slightly higher than pure H_5PMoV_2. The enhanced activity may be due to the improved redox property of POM-anions ascribed from the variation of the V state in the hybrid as demonstrated by ESR spectra.[23]

Interestingly, an extremely high TON of 2940 with still a considerably high yield of 29.4% can be obtained by charging 0.5 μmol (0.01 mol% vs. substrate) of the hybrid catalyst into the reactor (entry 6). In previous works, the TONs of different catalysts for oxidation of cyclohexane were usually in the range of 20-200, such as the homogeneous catalyst of di-iron-containing polyoxometalate γ-$SiW_{10}\{Fe(OH_2)\}_2O_{38}^{6-}$ with TON 53 and yield ca. 25.3%,[35] N,O-ligand-tethered dioxovanadium complex $[VO_2\{SO_3C(pz)_3\}]$ with TON 117 in the presence of HNO_3,[36] and $[VO(acac)_2(Hpz)]$ $HC(pz)_3$ immobilized on a polydimethylsiloxane membrane with TON up to 132.[25] Another typical early example is the hydrotris(pyrazol-1-yl)methane iron(II) complex immobilized on carbon material,[37] which offered the extremely high TON 5600 when the yield was inferior (11%), while TON was greatly lowered to 524 when the yield was enhanced to 20.8%. Recently, very high TONs and/or yields were reported by Pombeiro and coworkers over several complexes catalysts,[38-40] *i.e.*, the homogeneous heterometallic $Co^{III}_4Fe^{III}_2$ Schiff base complex (TON: 3570, yield: 26%), the Schiff base tetranuclear $Cu^{II}_2Fe^{III}_2$ complex (TON: 1100, yield: 44%), and the supported C-scorpionate iron(II) complex (yield/TON: 38%/2900 for the 1st run and 21%/1600 for the 2nd run). From above comparisons, it is drawn that the present newly obtained POM-based multi-cationic hybrid catalyst $[DPyAM(H_2)]_{1.25}PMoV_2$ is a highly active catalyst in terms of TON and yield.

After reaction, the catalyst $[DPyAM(H_2)]_{1.25}PMoV_2$ could be filtered from the reacted mixture for recovery; and a five-run catalyst recycling test was carried out under the optimal conditions, with the result shown in Fig. 3. Obviously, the reused catalysts exhibit no significant decrease in catalytic activity for the oxidation of cyclohexane compared with that of the fresh one; it maintains the high yield of ca. 32% and TON value of about 800. The XRD pattern (Fig. 2A, curve c) and IR spectrum (Fig. 2B, curve c) for the recovered catalyst are almost same as the fresh one. Further, the UV-vis spectra for the reused catalyst (Fig. 2C, curve c) also illustrates generally similar band to the fresh one, with a little redshift. These results together with the strong ESR signals for the recycled catalyst (Fig. 2D, curve c) reveal the durable structure of our hybrid catalyst in this reaction. Furthermore, the elemental analysis for the recovered catalyst finds C: 10.43%, N: 3.44%, H: 1.39% (weight percentage), very close to the data for the fresh catalyst, *i.e.*, no significantly enhanced C content is observed for the recycled catalyst. The durable structure and non-detection of the possible coke formation for the catalyst account for its superior recycling property.

In order to test the possible leaching of POM active species that is usually seen in POM-catalyzed H_2O_2-mediated oxidation, a hot filtration was carried out to remove the solid catalyst at the reaction time of 0.5 h, wherein 9% KA oil yield is obtained. The reaction was then proceeded for another 5.5 h with the filtrate, giving a slightly increased yield of 3%. The result on the one hand indicates the heterogeneity of our catalyst, on the other hand implies slight leaching of POM sites in the presence of H_2O_2, which may be responsible for the very slow decrease in activity during the catalyst recycling.

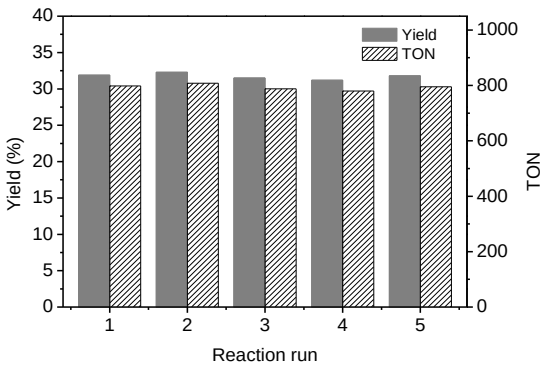

Fig. 3 Catalytic reusability of $[DPyAM(H_2)]_{1.25}PMoV_2$ for the oxidation of cyclohexane with H_2O_2. Reaction conditions: cyclohexane (5 mmol), catalyst (2 μmol), 30% H_2O_2 (10 mmol), 2,3-PDCA (0.3 mmol), CH_3CN (5 mL), 80 °C, 6 h.

A series of control catalysts were prepared and evaluated under the same conditions (Table 2) for the purpose to investigate the applicability of different IL-cations on this catalytic oxidation. When the tethered amino group on IL cation was varied to alkyl, cyano or carboxylic groups, the obtained analogous hybrids of $[DPyC_4]_{2.5}PMoV_2$, $[DPyCN]_{2.5}PMoV_2$ and $[DPyCOOH]_{2.5}PMoV_2$ are still able to cause liquid-solid heterogeneous catalytic systems, exhibiting the high product yields beyond 30% (entries 1-3). When the pyridinium-based IL was replaced with an imidazolium-based IL, the resultant hybrid $[DMim]_{2.5}PMoV_2$ also demonstrates the similarly high catalytic performance (entry 4). These features

View Article Online
DOI: 10.1039/C4RA15921G
RSC Advances

Table 2 Oxidation of cyclohexane with H_2O_2 over the catalysts with the varied IL-cations [a]

Entry	Structure of IL-cation in catalyst	Catalyst	Phenomenon	Yield[b][%]			Total TON[c]
				$C_6H_{11}OH$	$C_6H_{10}O$	Total	
1	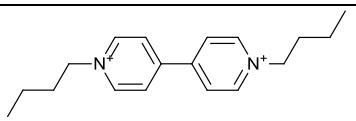	$[DPyC_4]_{2.5}PMoV_2$	heterogeneous	24.3	6.0	30.3	758
2	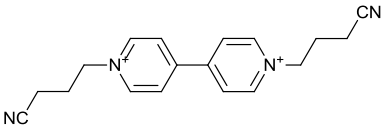	$[DPyCN]_{2.5}PMoV_2$	heterogeneous	24.9	6.7	31.6	790
3	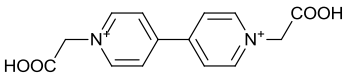	$[DPyCOOH]_{2.5}PMoV_2$	heterogeneous	26.3	5.7	32.0	800
4	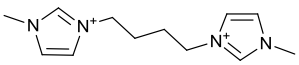	$[DMim]_{2.5}PMoV_2$	heterogeneous	25.4	6.9	32.3	808
5	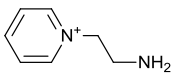	$[PyAM]_5PMoV_2$	homogeneous	19.4	8.1	27.5	688
6	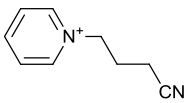	$[PyCN]_5PMoV_2$	homogeneous	22.4	6.0	28.4	710
7	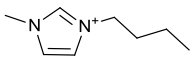	$[MimC_4]_5PMoV_2$	homogeneous	21.6	6.9	28.5	713
8	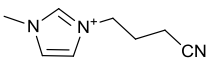	$[MimCN]_5PMoV_2$	homogeneous	23.0	4.7	27.7	693

[a] Reaction conditions (unless stated otherwise): cyclohexane (5 mmol), catalyst (2 μmol), 30% H_2O_2 (10 mmol), 2,3-PDCA (0.3 mmol), CH_3CN (5 mL), 80 °C, 6 h. Yields, TONs are determined by GC analysis (upon treatment with PPh_3). [b] Molar yield (%) based on substrate: moles of product (cyclohexanol + cyclohexanone) per 100 mol of cyclohexane. [c] Turnover number: moles of product (cyclohexanol + cyclohexanone) per mol of catalyst.

indicate a compositional flexibility of the series IL-dication-paired POM salts in catalyzing this oxidation reaction. However, for the monocationic ILs, the obtained hybrids (entries 5-8) result in homogeneous catalyses no matter what the functional groups are, though the product yields over these catalysts are considerably high (around 28%). Therefore, the featured structure of the multi- or di-IL-cations endows the hybrids to perform as the liquid-solid heterogeneous catalysts, while the monocationic counterparts behave homogeneously. In principle, the multi- or di-IL-cations have stronger electronic interaction with the high valent POM-anions than that of monocations,[41,42] which may be one major reason for the heterogeneous nature of the multi-cationic POM-based hybrid catalysts.

3.3. Influence of reaction conditions

Towards the optimization of the catalytic processes of cyclohexane oxidation over $[DPyAM(H_2)]_{1.25}PMoV_2$, the effects of a variety of key reaction factors were investigated, such as the amounts of catalyst, additive, solvent and H_2O_2, as well as the reaction time.

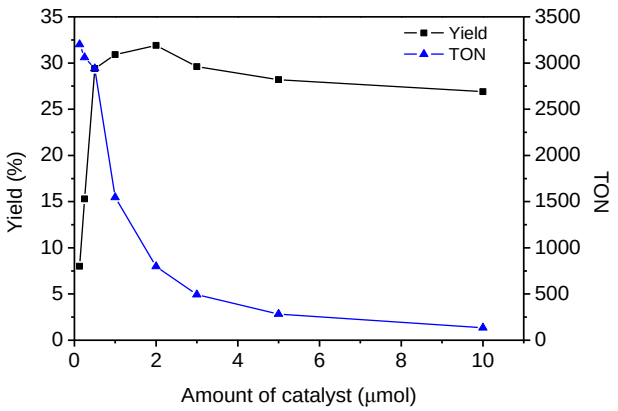

Fig. 4 Effect of the amount of catalyst $[DPyAM(H_2)]_{1.25}PMoV_2$ on cyclohexane oxidation. Reaction conditions: cyclohexane (5 mmol), 30% H_2O_2 (10 mmol), 2,3-PDCA (0.3 mmol), CH_3CN (5 mL), 80 °C, 6 h. Yields determined by GC analysis (upon treatment with PPh_3).

The effect of the catalyst amount on the overall yield and TON is investigated and plotted in Fig. 4. The product yield increases drastically in the region of low catalyst concentrations (0-0.5 μmol) before reaching a plateau. Afterwards, a slight

View Article Online
DOI: 10.1039/C4RA15921G
RSC Advances ARTICLE

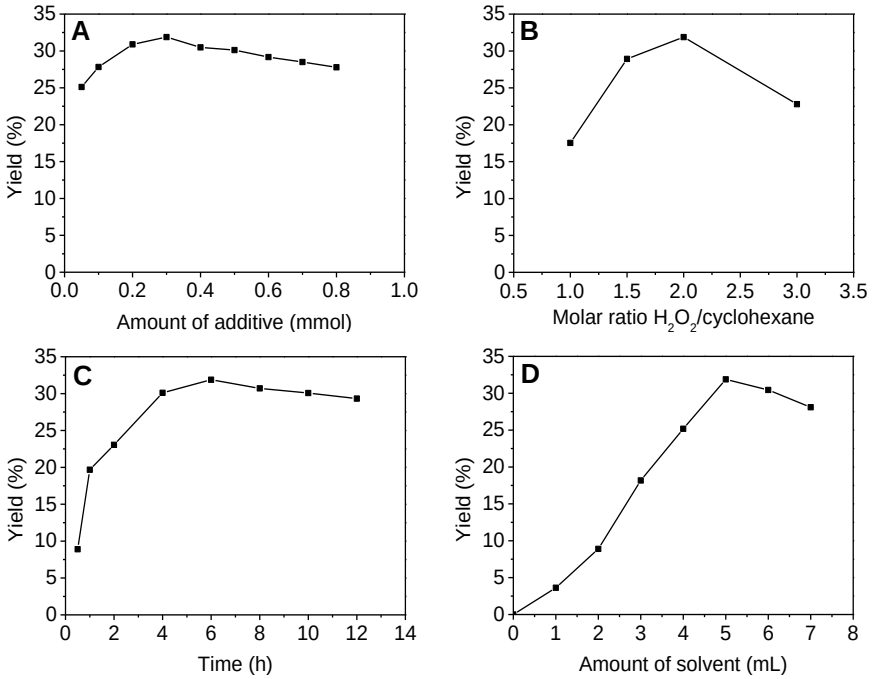

Fig. 5 Influences of reaction conditions on the oxidation of cyclohexane with H_2O_2 over the catalyst $[DPyAM(H_2)]_{1.25}PMoV_2$. (A) amount of acid additive. (B) molar ratio of H_2O_2 to cyclohexane. (C) reaction time. (D) amount of solvent. Reaction conditions: cyclohexane (5 mmol), 30% H_2O_2 (10 mmol), catalyst (2 μmol), 2,3-PDCA (0.3 mmol), CH_3CN (5 mL), 80 ^oC, 6 h. For each figure there is a specific parameter changed. Yields determined by GC analysis (upon treatment with PPh_3).

decrease happens at the higher catalyst amount over 2 μmol, due to the over-oxidation on the too much number of catalytically active sites. The highest yield of 31.9% is achieved with the catalyst amount of 2 μmol, which demonstrates that our system operates efficiently at a rather low catalyst loading (0.04 mol% vs. substrate). Such a catalyst loading is significantly lower than those commonly employed in most of the state-of-the-art systems for the oxidation of cyclohexane (up to 2 mol% vs. substrate).[43,44] The TON value is above 3000 at the initial reaction stage, and decreases with the increment of the catalyst amount. When the catalyst amount is 0.5 μmol, an extremely high TON of 2940 with still a considerably high yield of 29.4% can be obtained, implying an exceptional activity of this hybrid catalyst.

The effect of the amount of acidic additive pyrazine-2,3-dicarboxylic acid (2,3-PDCA) on product yield is shown in Fig. 5A. The yield increases along with the enhancement of 2,3-PDCA, and reaches the maximum of 31.9% when the amount of 2,3-PDCA raise up to 0.3 mmol. However, an excessive amount of 2,3-PDCA results in a decrease in yields, which suggests the creation of inactive coordination species when the excessive 2,3-PDCA interacts with the active metal centers competitively with the oxidant H_2O_2.[37] The effect of the amount of H_2O_2 (Fig. 5B) tells that increasing the molar ratio $n(H_2O_2)/n$(cyclohexane) up to 2.0 leads to the maximum product yield. Also, the excess amount of oxidant added is not suitable for the retaining of the wanted KA oil product, because a reverse effect on the yield is observed upon further increasing the oxidant amount due to over-oxidation. It should be pointed out that the optimal amount of H_2O_2 for the highest product yield is about twice as high as its stoichiometry, which could be attributed to the self-decomposition of H_2O_2. In fact, up to date the excess amount of H_2O_2 (H_2O_2/substrate: 2:1~5:1) is commonly used for oxidation of cyclohexane in previous reports.[45,46] The influence of the reaction time (Fig. 5C) indicates a continuous increase in yields from 19.7% to 31.9% when the time is from 1 h to 6 h. Further increasing the reaction time causes the decline of yields, implying occurrence of deep oxidation of KA oil at the too much elongated reaction time. The amount of solvent acetonitrile in the reaction mixture also significantly affects the yield (Fig. 5D). In the absence of acetonitrile, rare products are formed. This is understandable because the distinct phase separation is observed between the oxidant-involving aqueous phase and the organic substrate, which limits interactions among substrate, oxidant and catalyst. The yield remarkably increases with the raise of the solvent amount up to 5 mL, where the maximum yield is achieved. With a further addition of the solvent, the yield decreases, corresponding to the well-known dilution effect for substrates and/or intermediates.

3.4. Understanding of the catalytic behavior

The reaction pathway for cyclohexane oxidation has been reported and in most cases the reaction goes through a radical mechanism.[47] In order to examine the general type of mechanism involved in our catalytic oxidation of cyclohexane, we performed the reaction in the presence of radical traps of $CBrCl_3$, BHT or Ph_2NH (Table 1, entry 7), which shows no product. The result strongly indicates that the present oxidation reaction proceeds *via* a free-radical mechanism.[45] Accordingly, the possible mechanism of $[DPyAM(H_2)]_{1.25}PMoV_2$-catalyzed cyclohexane oxidation

View Article Online
DOI: 10.1039/C4RA15921G
RSC Advances

with H_2O_2 is proposed in Scheme 3. In the initial period of the reaction, the vanadium active species in the hybrid catalyst reacts with H_2O_2 to generate the hydroperoxyl radical HOO ; meanwhile, the high valent vanadium (V) is reduced to vanadium (IV), in agreement with the previous suggestion[31]. After that, the second hydrogen peroxide molecule attacks the transition state of vanadium (IV) to generate the hydroxyl radical HO ; whilst the vanadium (IV) is oxidized reversely to the higher oxidation state vanadium (V), which thus completes the catalytic cycle. Within the cycle, the substrate cyclohexane molecule reacts with the resulting radicals HOO · and HO · to give the products of cyclohexanol and cyclohexanone *via* the known further route.[48,49]

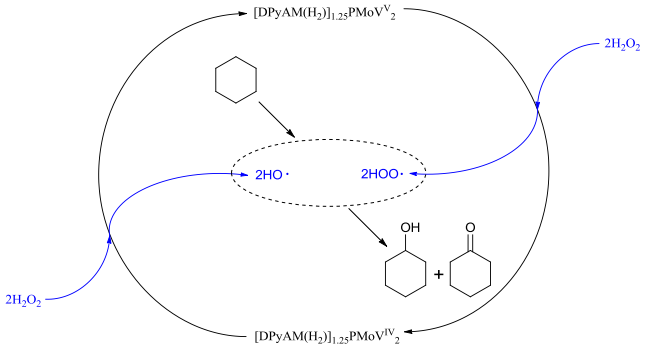

Scheme 3 Proposed catalytic mechanism for $[DPyAM(H_2)]_{1.25}PMoV_2$-catalyzed oxidation of cyclohexane with H_2O_2.

4. Conclusions

In this study, we develop a new catalyst by pairing the task-specifically designed IL-cation of N,N'-bis-2-aminoethyl-4,4'-bipyridinium with the Keggin-structured vanadium-substituted polyoxometalate anion $PMo_{10}V_2O_{40}^{5-}$. Systematic characterizations for composition and structure demonstrate that the catalyst is the POM-based multi-cationic hybrid $[DPyAM(H_2)]_{1.25}PMoV_2$. In the oxidation of cyclohexane with H_2O_2, the catalyst offers an exceptional activity with not only remarkable TON value but also relative high yield for KA oil (cyclohexanol + cyclohexanone). The featured structure of the multi-cations in the hybrid results in its solid-state nature and heterogeneous property in this oxidation reaction. Overall, the catalyst is stable and keeps constant yield during the tested 5 cycles, thus providing an efficient heterogeneous catalysis strategy for the oxidation of cyclohexane with hydrogen peroxide.

Acknowledgements

The authors thank the National Natural Science Foundation of China (Nos. 21136005, 21303038 and 21476109), Jiangsu Province Science Foundation for Youths (No. BK20130921), Specialized Research Fund for the Doctoral Program of Higher Education (No. 20133221120002), and the Project of Priority Academic Program Development of Jiangsu Higher Education Institutions (PAPD).

Notes and references

State Key Laboratory of Materials-Oriented Chemical Engineering, College of Chemistry and Chemical Engineering, Nanjing Tech University, Nanjing 210009, P. R. China. Tel: +86-25-83172264. Fax: +86-25-83172261. E-mail: njutzhouyu@njtech.edu.cn (Y. Zhou); junwang@njtech.edu.cn (J. Wang).

† Electronic Supplementary Information (ESI) available: Details of the synthesis and structure formulas of various control catalysts, ^1H NMR of ionic liquid precursor $[DPyAM]Br_2 2HBr$ and the hybrid $[DPyAM(H_2)]_{1.25}PMoV_2$ are provided. See DOI: 10.1039/b000000x/

1 J. A. Labinger, *J. Mol. Catal. A: Chem.*, 2004, **220**, 27-35.
2 R. H. Crabtree, *Chem. Rev.*, 1995, **95**, 987-1007.
3 M. M. A. Pereira, *Curr. Org. Chem.*, 2012, **16**, 1680-1710.
4 A. Ranoux, K. Djanashvili, I. W. C. E. Arends and U. Hanefeld, *RSC Adv.*, 2013, **3**, 21524-21534.
5 S. S. Reddy, B. David Raju, A. H. Padmasri, P. K. Sai Prakash and K. S. Rama Rao, *Catal. Today*, 2009, **141**, 61-65.
6 D. Alberico, M. E. Scott and M. Lautens, *Chem. Rev.*, 2007, **107**, 174-238.
7 F. P. Canhota, G. C. Salomão, N. M. F. Carvalho and O. A. C. Antunes, *Catal. Commun.*, 2008, **9**, 182-185.
8 H. Li, Y. She and T. Wang, *Chem. Sci. Eng.*, 2012, **6**, 356-368.
9 J. Tong, L. Bo, X. Cai, H. Wang, Q. Zhang and L. Su, *Ind. Eng. Chem. Res.*, 2014, **53**, 10294-10300.
10 M. J. L. Kishore and A. Kumar, *Ind. Eng. Chem. Res.*, 2007, **46**, 4787-4798.
11 I. V. Kozhevnikov, *Chem. Rev.*, 1998, **98**, 171-198.
12 M. M. Q. Simoes, C. M. M. Conceição, J. A. F. Gamelas, P. M. D. N. Domingues, A. M. V. Cavaleiro, J. A. S. Cavaleiro, A. J. V. Ferrer-Correia and R. A. W. Johnstone, *J. Mol. Catal. A: Chem.*, 1999, **144**, 461-468.
13 K. Kamata, K. Yonehara, Y. Nakagawa, K. Uehara and N. Mizuno, *Nat. Chem.*, 2010, **2**, 478-483.
14 W. Trakarnpruk and J. Jatupisarnpong, *Appl. Petrochem. Res.*, 2013, **3**, 9-15.
15 J. Jatupisarnpong and W. Trakarnpruk, *Mendeleev Commun.*, 2012, **22**, 152-153.
16 W. Trakarnpruk and W. Kanjina, *J. Met. Mater. Miner.*, 2013, **23**, 31-35.
17 Y. Liu, K. Murata and M. Inaba, *Catal. Commun.*, 2005, **6**, 679-683.
18 Y. Leng, J. Wang, D. Zhu, L. Shen, P. Zhao and M. Zhang, *Chem. Eng. J.*, 2011, **173**, 620-626.
19 P. Zhao, M. Zhang, Y. Wu and J. Wang, *Ind. Eng. Chem. Res.*, 2012, **51**, 6641-6647.
20 G. Chen, Y. Zhou, P. Zhao, Z. Long and J. Wang, *ChemPlusChem*, 2013, **78**, 561-569.
21 G. Chen, Y. Zhou, Z. Long, X. Wang, J. Li and J. Wang, *ACS Appl. Mater. Inter.*, 2014, **6**, 4438-4446.
22 Y. Zhou, G. Chen, Z. Long and J. Wang, *RSC Adv.*, 2014, **4**, 42092-42113.
23 Y. Leng, H. Ge, C. Zhou and J. Wang, *Chem. Eng. J.*, 2008, **145**, 335-339.
24 Y. Leng, P. Zhao, M. Zhang and J. Wang, *J. Mol. Catal. A: Chem.*, 2012, **358**, 67-72.

View Article Online
DOI: 10.1039/C4RA15921G
RSC Advances ARTICLE

25 T. F. S. Silva, T. C. O. Mac Leod, L. M.D.R.S. Martins, M. F. C. Guedes da Silva, M. A. Schiavon and A. J. L. Pombeiro, *J. Mol. Catal. A: Chem.*, 2013, **367**, 52-60.
26 G. B. Shul'pin, *J. Mol. Catal. A: Chem.*, 2002, **189**, 39-66.
27 M. Langpape, J. M. M. Millet, U. S. Ozkan and M. Boudeulle, *J. Catal.*, 1999, **181**, 80-90.
28 H. Benaissa, P.N.Davey, Y.Z. Khimyak and I.V. Kozhevnikov, *J. Catal.*, 2008, **253**, 244-252.
29 C. Rocchiccioli-Deltcheff and M. Fournier, *J. Chem. Soc. Faraday Trans.*, 1991, **87** (24), 3913-3920.
30 L. S. Felices, P. Vitoria, J. M. Gutiérrez-Zorrilla, S. Reinoso, J. Etxebarria and L. Lezama, *Chem. Eur. J.*, 2004, **10**, 5138-5146.
31 P. Zhao, J. Wang, G. Chen, Y. Zhou and J. Huang, *Catal. Sci. Technol.*, 2013, **3**, 1394-1404.
32 G. Ranga Rao and T. Rajkumar, *Catal. Lett.*, 2008, **120**, 261-273.
33 T. Yamase, *Chem. Rev.*, 1998, **98**, 307-325.
34 T. Sakamoto, T. Takagaki, A. Sakakura, Y. Obora, S. Sakaguchi and Y. Ishii, *J. Mol. Catal. A: Chem.*, 2008, **288**, 19-22.
35 N. Mizuno, I. Kiyoto, C. Nozaki and M. Misono, *J. Catal.*, 1999, **181**, 171-174.
36 T. F. S. Silva, K. V. Luzyanin, M. V. Kirillova, M. F. Guedes da Silva, L. M.D.R.S. Martins and A. J. L. Pombeiro, *Adv. Synth. Catal.*, 2010, **352**, 171-187.
37 L. M.D.R.S. Martins, M. Peixoto de Almeida, S. A. C. Carabineiro, J. L. Figueiredo and A. J. L. Pombeiro, *ChemCatChem*, 2013, **5**, 3847-3856.
38 D. S. Nesterov, E. N. Chygorin, V. N. Kokozay, V. V. Bon, R. Boča, Y. N. Kozlov, L. S. Shul'pina, J. Jezierska, A. Ozarowski, A. J. L. Pombeiro and G. B. Shul'pin, *Inorg. Chem.*, 2012, **51**, 9110-9122.
39 L. M.D.R.S. Martins, A. Martins, E. C.B.A. Alegria, A. P. Carvalho and A. J. L. Pombeiro, *Appl. Catal. A-Gen.*, 2013, **464-465**, 43-50.
40 O. V. Nesterova, E. N. Chygorin, V. N. Kokozay, V. V. Bon, I. V. Omelchenko, O. V. Shishkin, J. Titiš, R. Boča, A. J. L. Pombeiro and A. Ozarowski, *Dalton Trans.*,2013, **42**, 16909-16919.
41 T. Payagala, J. Huang, Z. S. Breitbach, P. S. Sharma and D. W. Armstrong, *Chem. Mater.*, 2007, **19**, 5848-5850.
42 J. L. Anderson, R. Ding, A. Ellern and D. W. Armstrong, *J. Am. Chem. Soc.*, 2005, **127**, 593-604.
43 K. T. Mahmudov, M. N. Kopylovich, M. F. Guedes da Silva, P. J. Figiel, Y. Y. Karabach and A. J. L. Pombeiro, *J. Mol. Catal. A: Chem.*, 2010, **318**, 44-50.
44 T. F. S. Silva, M. F. Guedes da Silva, G. S. Mishra, L. M.D.R.S. Martins and A. J. L. Pombeiro, *J. Organomet. Chem.*, 2011, **696**, 1310-1318.
45 M. Peixoto de Almeida, L. M.D.R.S. Martins, S. A. C. Carabineiro, T. Lauterbach, F. Rominger, A. S. K. Hashmi, A. J. L. Pombeiro and J. L. Figueiredo, *Catal. Sci. Technol.*, 2013, **3**, 3056-3069.
46 B. Sarkar, P. Prajapati, R. Tiwari, R. Tiwari, S. Ghosh, S. S. Acharyya, C. Pendem, R. K. Singha, L. N.S. Konathala, J. Kumar, T. Sasaki and R. Bal, Green Chem., 2012, **14**, 2600-2606.
47 A. M. Kirillov and G. B. Shul'pin, *Coord. Chem. Rev.*, 2013, **257**, 732-754.
48 M. V. Kirillova, Y. N. Kozlov, L. S. Shul'pina, O. Y. Lyakin, A. M. Kirillov, E. P. Talsi, A. J. L. Pombeiro and G. B. Shul'pin, *J. Catal.*, 2009, **268**, 26-38.
49 M. V. Kirillova, M. L. Kuznetsov, V. B. Romakh, L. S. Shul'pina, J. J. R. Fraústo da Silva, A. J. L. Pombeiro and G. B. Shul'pin, *J. Catal.*, 2009, **267**, 140-157.